International Journal of Multidisciplinary and Innovative Research

ISSN(print): 3050-6883, ISSN(online): 3050-6891

Volume 03 Issue 01 January 2026

DOI: 10.58806/ijmir.2026.v3i1n11

Page No: 88-99

Biomechanical Evaluation of An Innovative Triple Abutment System in Ceramic Versus Titanium Implants : A Finite Element Analysis

Luciana S. Colepícolo[1], **Maria Auxiliadora M. Martinez**[2], **Luís Otávio M. Cota**[3], **Rafael Paschoal E. Lima**[4], **Fernando O. Costa**[5]

[1,2,3,4,5]Faculty of Dentistry, Federal University of Minas Gerais, Brazil.

ORCID ID

[1]https://orcid.org/0000-0003-10546608
[2]https://orcid.org/0009-0006-2823-3748
[3]https://orcid.org/0000-0003-4343-3845
[4]https://orcid.org/0000-0003-1517-5842
[5] https://orcid.org/0000-0002-7687-1238

ABSTRACT

Aim: To compare the biomechanical behavior of an innovative triple abutment (TA) with a hyperbolic paraboloid geometry, designed to support three dental crowns on a single implant, using finite element analysis under two conditions: a ceramic model with a zirconia implant and metal–ceramic crowns (TA ceramic) and a conventional model with a titanium implant and metal–ceramic crowns (TA Ti).

Materials and Methods: Three-dimensional finite element models were developed to evaluate stress and microstrain distribution in peri-implant bone, as well as stress distribution in the abutment, UCLA abutment, implant body, and retaining screw under axial (250 N) and oblique (100 N) loading. Each model included a bone block representing the region from the second premolar to the first molar in the upper right quadrant, incorporating a Morse taper implant.

Results: The TA ceramic model showed 10–20% higher stress in prosthetic components compared with the TA Ti model. However, differences in stress and microstrain within the surrounding bone were below 5%, remaining within clinically acceptable limits.

Conclusions: Both ceramic and titanium implants combined with the TA abutment demonstrated favorable biomechanical performance. Implant material selection may therefore be guided by clinical priorities, particularly esthetic requirements, without significantly compromising mechanical behavior.

KEYWORDS: zirconia; dental implant-abutment design; finite element analysis; Mechan transduction.

ARTICLE DETAILS

Published On:
28 January 2026

Available on:
https://ijmir.com

1.0 INTRODUCTION

The evolving concept of osseointegration as a dynamic process requires deeper insights into the biomechanical principles governing load distribution. A novel triple prosthetic abutment (TA) featuring a hyperbolic paraboloid geometry was recently introduced by Colepícolo et al. [1], together with a new framework referred to as Biodynamically Optimized Peri-implant Tissue (BOPiT). In this system, a single implant, combined with the TA, supports three dental crowns, demonstrating remarkably satisfactory outcomes in terms of peri-implant tissue preservation in a series of 15 cases, with clinical follow-up of up to 12 years [1].

Within this context, the use of ceramic implants and crowns in the rehabilitation of partially edentulous patients has become a significant advancement in contemporary implant dentistry [2-4]. Specifically, the use of zirconia-based ceramics (ZrO_2) as a biomaterial has seen substantial growth, driven by several desirable properties, including: (i) excellent mechanical resistance to wear and fracture (compressive strength around 2000 MPa) [5]; (ii) favorable behavior against crack propagation, since the martensitic

phase transformation under surface stress acts as a crack-arrest mechanism [6]; (iii) ease of processing through digital manufacturing techniques such as CAD/CAM systems used for fabricating crowns and fixed partial dentures [2,7,8]; and (iv) superior aesthetics [9,10].
From an esthetic perspective, ceramic implants exhibit a whitish coloration and some degree of translucency, rendering them nearly indistinguishable from natural teeth—an especially advantageous feature in patients with a thin gingival biotype [7, 9, 10]. In such cases, the grayish hue of metallic implants, particularly in high smile lines, may compromise the final esthetic outcome [8].
Furthermore, ceramic implants are hypoallergenic, representing a safe alternative for patients with metal hypersensitivity [11]. Although titanium allergy prevalence is considered low (~0.6%), there is evidence of increased risk of adverse reactions in patients exhibiting postoperative hypersensitivity symptoms, such as unexplained inflammatory responses or early implant failures [3,12]. Another notable advantage of ceramic implants is their lower thermal conductivity compared to metallic counterparts, potentially reducing the oral sensitivity and discomfort often reported by patients [3, 13].

Despite being considered an emerging technology, ceramic implants have shown promising results regarding long-term success rates and durability, supporting their growing adoption. However, further studies are necessary to validate their clinical and biomechanical benefits.

In this context, the present study aims to compare the biomechanical performance, specifically stress and strain distribution via finite element analysis (FEA) of the TA abutment in two distinct scenarios: (i) a model using a ZrO_2 implant and metal-ceramic crowns (TA ceramic); and (ii) a conventional model comprising a titanium implant with metal-ceramic crowns (TA Ti).

It is noteworthy that FEA is widely recognized as a robust methodology for evaluating stresses and deformations in complex three-dimensional structures [14,15].

2.0 MATERIALS AND METHODS

2.1. Overview of the TA System

The innovative TA features a hyperbolic paraboloid geometric design along its entire length, exhibiting a doubly ruled surface (composed of multiple straight lines whose combination forms the surface itself), generally saddle-shaped. A hyperbolic paraboloid opens downward along one axis and upward along another. The TA design provides high rigidity by reducing bending stresses and equalizing forces. Vectorial loads are minimized, preventing the traditional transverse coordinate axis that contributes to early bone loss in the implant abutment connection área [1]. These designs represent the interaction between biological and mathematical phenomena. Further information on the geometry and biomechanics of the TA was detailed in Colepicolo et al. [1].

Thus, TA components function as multiple mechanical load organizers and can support three crowns on a single implant, featuring an innovative geometric design that is fully passive (without welding) (Figure 1). This system is secured by multiple patents across different regions (Brazil: 112020009609A2; India: 517585; Europe: 17932138.5; USA: 11.701.206 B2).

2.2 Experimental study

This in vitro experimental study employed a bone model derived from computed tomography (CT) scans of a dentate maxilla (covering the region from the second premolar to the first molar). The model represented the upper arch with dimensions of 18.0 mm in height, 19.0 mm mesiodistally, and 15.0 mm buccolingually, and was classified as Type 3 bone (with a 1.0 mm cortical layer surrounding trabecular bone).

All materials were modeled with isotropic and elastic properties using Young's modulus (E) and Poisson's ratio (ν), based on the parameters described by Capatti et al. [[16]. For materials evaluated according to the Mohr-Coulomb and Von Mises criteria, both tensile and compressive yield strengths were incorporated. The mechanical properties of zirconia were based on data reported by Guilardi et al. [17] and Fiorillo et al. [8]. Table 1 lists the material properties used.

Two finite element models were constructed: one representing the TA ceramic configuration (a model using a ZrO_2 implant and metal-ceramic crowns) and the other representing the TA Ti configuration (a conventional model comprising a titanium implant with metal-ceramic crowns). Both models used a single Morse-taper implant (3.75 × 10.0 mm, Dentoflex, Brazil), placed approximately 2 mm below the cortical surface. The prosthetic crowns were standardized to 15 mm in height. The geometries were created using Fusion 360 software (Autodesk Company, San Francisco, California, USA) and exported to ANSYS (ANSYS Inc., Canonsburg, Pennsylvania, USA) for FEA simulations (Figure 2).

Simulations were carried out in two phases: initial bolt pretensioning followed by occlusal loading. Two loading conditions were applied [18, 19]: (1) an axial load of 250 N evenly distributed across the occlusal fossae and (2) an oblique load of 100 N applied at a 45° angle in the lingual direction.

Bolt pretensioning was modeled using the "bolt pretension" element in ANSYS. The preload was adjusted to 65–75% of the titanium yield strength (520–600 MPa), resulting in a preload of 300 N for the abutment screw and 150 N for the prosthetic screw.

Implant and occlusal contacts were modeled as frictional ($\mu = 0.2$), while the abutment-to-bone contact was considered frictionless. All other contacts were defined as bonded. A preliminary simulation confirmed the absence of residual pre-stress due to contact interference.

Despite model simplifications (e.g., homogeneous and isotropic bone), the FEA approach used is well supported in the literature [20-22] and remains effective for evaluating stress distribution. The models were assessed using maximum (tensile) and minimum (compressive) principal stresses, Von Mises stresses, and strain magnitudes.

Mesh convergence was verified to ensure solution accuracy. Second-order tetrahedral elements were used for mesh construction, as they better represent the complex three-dimensional geometry of implants, teeth, and bone. The final mesh consisted of 736,221 nodes and 441,490 elements.

Additionally, the support reactions obtained from the FEA models were analyzed to verify the correct implementation of loading conditions and to interpret the mechanical behavior of the simulated system. As the goal was to compare the TA ceramic and TA ti configurations, it was essential that the support reactions be equivalent in both models, indicating that the boundary conditions and loading constraints were consistently applied.

3. RESULTS

Table 2 presents the maximum stress values observed in the components of both models under axial (250 N) and oblique (100 N) loading. Higher peak stresses were observed in the TA ceramic model, particularly in the implant, mini abutment/UCLA, and screw, when compared to the TA Ti model. The observed increases ranged from approximately 10% to 20%, which is consistent with the higher stiffness of zirconia relative to titanium

Table 3 shows the results for stress and microstrain in the bone structure under both loading scenarios. The differences between the two models were less than 5%, which is considered clinically acceptable and supports the potential viability of ceramic-based structures.

These results are also illustrated in Figure 3, where areas of maximum stress are shown in red and minimum stress in blue.

Figure 4 displays the force application points (a), as well as the mesh convergence graphs for both models under oblique (b, c) and axial (d, e) loading. It can be observed that the TA ceramic model demonstrates convergence with mesh refinement, and stress variations remain within the 5% range, indicating no significant impact on the results.

Table 4 reports the support reactions for both FEA models, confirming the correct application of loads and verifying that the boundary conditions were consistent across both simulations.

Figure 5 illustrates a clinical and radiographic presentation of the use of TA Ti in an 10-year follow-up [1].

4.0 DISCUSSION

This study demonstrated that, overall, the biomechanical behavior of the TA ceramic model was comparable to that of the TA Ti model. The stresses observed in the TA ceramic model were higher for most components, with the greatest difference seen in the implant (15%), and the highest overall increase (18.4%) occurring in the prosthetic screw—potentially indicating a higher likelihood of failure in this component. Nevertheless, these results were expected due to the higher stiffness of ZrO_2 (elastic modulus of 205 GPa compared to 105 GPa for titanium), and these stress levels remain within acceptable limits.

In the evaluation of the bone structure, the stress differences between models were below 5%, which is also attributed to the higher elastic modulus of zirconia, leading to increased rigidity and lower stress dissipation. In this simulation, these differences were not sufficient to cause material yielding or failure, as the compressive strength of zirconia exceeds the yield strength of titanium by approximately 150%.

Thus, aligned with current trends favoring all-ceramic restorations in the rehabilitation of edentulous spaces with implants, the innovative TA abutment may be employed in conjunction with the advantages of ZrO_2, including: superior mechanical properties [5, 6]; enhanced manufacturability using CAD/CAM systems [2,7,8]; and superior esthetics, with no shadowing in cervical areas—particularly relevant in patients with a thin gingival biotype. [9,10]

However, a potential drawback of ZrO_2-based structures has been reported: early studies indicate that their resistance to loosening (disconnection) is inferior to that of titanium, although appropriate surface treatments may help mitigate this issue [8, 23, 24].

It is also worth noting that the use of the TA abutment is supported by the Biodynamics Optimized Peri-Implant Tissue (BOPiT) concept, which integrates principles from bone mechanotransduction [25, 26], biotensegrity [27, 28], and mechanobiology [27, 29, 30]. BOiPT merges mathematical and biophysical principles related to force vectors and load distribution, enabling dynamic and differentiated transmission of forces to peri-implant tissues through the biologically active geometry of the TA abutment. Its advantages include: reduced stress concentration at the implant platform and screw, the ability to support overdentures with a single implant, viability in angled implant situations, full passivity, and ease of hygiene (the prophylactic parabolic emergence profile of the TA allows regular dental flossing due to its segmented tripod configuration) [1].

In this study, the stresses experienced by the ceramic structures were predominantly compressive, owing to the direction of masticatory forces, which favors structural safety. Changes in geometry, abutment angulation, crown height, or load magnitude/orientation could induce higher tensile stresses, potentially leading to material failure, given that the tensile strength of yttria-stabilized zirconia is lower than the yield strength of titanium.

Despite these considerations, for both loading conditions analyzed, the behavior of the TA ceramic model was similar to that of the TA Ti model, with no significant failure regions identified due to material differences.

FEA is a numerical technique used to estimate mechanical characteristics by transforming partial differential equations into algebraic systems [8,31]. Its key feature is discretization, achieved by creating a mesh composed of primitive elements—triangles and quadrilaterals for 2D domains, tetrahedrons and hexahedrons for 3D domains. The solution is expressed as a linear combination of shape functions, sometimes approximated to minimize global solution error [8, 31, 32].

This study is limited by its *in vitro* nature; FEA is widely regarded as a valuable tool for preclinical evaluation, particularly for predicting unfavorable mechanical scenarios [14, 15, 18]. However, it is important to emphasize that *in vitro* testing contributes significantly to understanding the mechanical behavior of implantable materials, yet it does not necessarily reflect the outcomes observed in clinical follow-ups due to inherent limitations. Specifically, such tests do not simulate physiological conditions, such as temperature fluctuations, the presence of oral fluids, occlusal interferences, bruxism-related factors, or the dynamic action of masticatory muscles [33]. As with other methodologies, FEA presents certain limitations. Therefore, future research should integrate FEA with long-term randomized clinical trials to validate these findings, taking into account variables such as patient-specific bone morphology and implant geometries.

Thus, the biomechanical performance of the TA ceramic model was comparable to that of the TA Ti model. Therefore, the indication of ceramic or titanium implants using the innovative TA abutment may be guided by clinical criteria tailored to the specific demands of each case, particularly those with higher aesthetic requirements. The findings indicate that the TA with a hyperbolic paraboloid geometry is biomechanically viable for both ceramic and titanium implants. Although the ceramic version exhibited higher stress levels in the prosthetic components, this difference does not compromise clinical safety. Bone stress values were similar between models, remaining within acceptable limits. Therefore, material selection may be based on aesthetic demands or individual sensitivities, without functional compromise. Thus, the proposed TA expands rehabilitation options by enabling the use of a single implant to support multiple crowns.

ABBREVIATIONS

Biodynamically Optimized Peri-implant Tissue (BOPiT); finite element analysis (FEA) ; innovative triple abutment (TA); model using a ZrO_2 implant and metal-ceramic crowns (TA ceramic); model comprising a titanium implant with metal-ceramic crowns (TA Ti) ; zirconia-based ceramics (ZrO_2) ;

ACKNOWLEDGMENTS

Dentoflex, São Paulo, Brazil, for the support with implants and other structures used in the fabrication of the models.

REFERENCES

1) Colepícolo LS, Mourão Martinez MA, Rodrigues AA, Baeta LS, Costa FO. The innovative double or triple dental abutment-implant: Case study with a 3- to 12-year follow-up. Clin Adv Periodontics. 15, no.3 (2025):200-212. doi: 10.1002/cap.10300.
2) Gautam C, Joyner J, Gautam A, Rao J, Vajtai R. Zirconia based dental ceramics: structure, mechanical properties, biocompatibility and applications. *Dalton Transactions* 45, no. 48 (2016): 19194-19205. doi: 10.1039/c6dt03484e.
3) C. Bollen, G. Hakobayan, M. Jörgens. One-piece versus two-piece ceramic dental implants. *British Dental Journal* 236, no. 5 (2024) : 383-387. doi: 10.1038/s41415-024-7123-3.
4) C. Bollen. Zirconia: the material of choice in implant dentistry? An update. *Journal of Dentistry and Health Oral, Disorders and Therapy* 6, (2017): 172-175.
5) F.H. Schünemann, M.E. Galárraga-Vinueza, R. Magini, M. Fredel, F. Silva, J.C.M. Souza, et al. Zirconia surface modifications for implant dentistry. *Materials Science & Engineering. C, Materials for Biological Applications* 98 (2019): 1294-1305. doi: 10.1016/j.msec.2019.01.062.
6) T. Miyazaki, T. Nakamura, H. Matsumura, S. Ban, T. Kobayashi. Current status of zirconia restoration. *Journal of Prosthodontics Research* 57, no. 4 (2013): 236-261. doi: 10.1016/j.jpor.2013.09.001.
7) S.Ban. Chemical durability of high translucent dental zirconia. *Dental Materials Journal* 39, no. 5 (2020): 12-23. doi: 10.4012/dmj.2019-109.
8) L. Fiorillo, D. Milone, D. D'Andrea, D. Santonocito, G. Risitano, G. Cervino, et al. Finite element analysis of zirconia dental implant. *Prosthesis* 4 (2022)490–499. doi: 10.3390/prosthesis4030040.
9) N. Cionca, D. Hashim, A. Mombelli. Zirconia dental implants: where are we now, and where are we heading? *Periodontology 2000* 73, no.1 (2017): 241-58. doi: 10.1111/prd.12180.
10) I. Comisso, S. Arias-Herrera, S. Gupta. Zirconium dioxide implants as an alternative to titanium: A systematic review. *Journal of Clinical Experimental Dentistry* 13, no. 5 (2021): e511-e519. doi: 10.4317/jced.58063.

11) P. Kubasiewicz-Ross, M. Dominiak, T. Gedrange, U.U. Botzenhart. Zirconium: the material of the future in modern implantology. *Advances Clinical Experimental Medicine* 26, no. 3 (2017): 533-537. doi: 10.17219/acem/63794.
12) A. Sicilia, S. Cuesta, G. Coma, I. Arregui, C. Guisasola, E. Ruiz, A. et al. Titanium allergy in dental implant patients: a clinical study on 1500 consecutive patients. *Clinical Oral Implants Research* 19, no. 8 (2008): 823-835. doi: 10.1111/j.1600-0501.2008.01544.x.
13) M. Montazerian, E.D. Zanotto. Bioactive and inert dental glass-ceramics. *Journal of Biomedical Materials Research A* 105 (2017): 619-639. doi: 10.1002/jbm.a.35923.
14) G. Mehdi, A. Belarbi, B. Mansouri, Z. Azari. Numerical study of effect of elastomeric stress absorbers on stress reduction in bone-dental implant interface. *Journal of Applied Oral Science* 23, no.1 (2015): 87-93. doi: 10.1590/1678-775720140086.
15) M.B. Toniollo, M.D.S. Sá, F.P. Silva, G.R. Reis, A.P. Macedo, A.S.S.D. Terada. Comparison of conventional and pontic fixed partial dentures over implants using the finite element method: Three-dimensional analysis of cortical and medullary bone stress. *Journal of Oral Implantology* 46, no. 3 (2020):175-181. doi: 10.1563/aaid-joi-D-19-00115.
16) R.S. Capatti, M.S. Barboza, A.N. da Gama Antunes, D.D. Oliveira, P.I. Seraidarian. Viability of Maxillary Single Crowns Supported by 4-mm Short Implants: A Finite Element Study. *International Journal of Oral Maxillofacial Implants* 35 (2020): e41-e50. doi: 10.11607/jomi.6784
17) L.F. Guilardi, G.K.R. Pereira, V.F. Wandscher, M.P. Rippe, L.F. Valandro. Mechanical behavior of yttria-stabilized tetragonal zirconia polycrystal: Effects of different aging regimens. *Brazilian Oral Research* 31 (2017): e94. doi: 10.1590/1807-3107bor-2017.vol31.0094.
18) V.E. de Souza Batista, F.R. Verri, D.A. Almeida, J.F. Santiago Jr, C.A. Lemos, E.P. Pellizzer. Finite element analysis of implant-supported prosthesis with pontic and cantilever in the posterior maxilla. *Computers Methods Biomechanical Biomedical Engineering* 20, no. 6 (2017): 663-670. doi: 10.1080/10255842.2017.1287905.
19) K.T.S. Tsumanuma, R.A. Caldas, I.D. Silva, M.E. Miranda, W.C. Brandt, R.P. Vitti. Finite element analysis of stress in anterior prosthetic rehabilitation with zirconia implants with and without cantilever. *European Journal of Dentistry* 15, no. 4 (2021): 669-674. doi: 10.1055/s-0041-1727544.
20) F.R. Verri, V.E. Batista, J.F. Santiago Jr, D.A. Almeida, E.P. Pellizzer. Effect of crown-to-implant ratio on peri-implant stress: a finite element analysis. *Materials Science Engineering C Materials for Biological Applications* 45 (2014): 234-240. doi: 10.1016/j.msec.2014.09.005.
21) A. Boukhlif, A. Merdji, N. Della.Numerical evaluation of biomechanical stresses in dental bridges supported by dental implants. J*ournal of Biomimetics, Biomaterials and Biomedical Engineering* 37, no.10 (2018): 43-54.
22) N. Husain. Load bearing capacity of 3-unit screw-retained implant-supported fixed dental prostheses with a mesial and distal cantilever on a single implant: A comparative in vitro study. *Journal of the Mechanical Behavior of Biomedical Materials* 151 (2024): 106395. doi: 10.1016/j.jmbbm.2024.106395.
23) Z. Petrović, A. Šarić, I. Despotović, J. Katić, R. Peter, M. Petravić, M. et al. A new insight into coating's formation mechanism between TiO_2 and alendronate on titanium dental implant. *Materials* 13 (2020): 3220. doi: 10.3390/ma13143220
24) H. Dong, H. Liu, N. Zhou, Q. Li, G. Yang, L. Chen, Y. Mou. Surface modified techniques and emerging functional coating of dental implants. *Coatings* 10 (2020): 1012.
25) Y. Ban, Y.Y. Wu, T. Yu, N. Geng, Y.Y. Wang, X.G. Liu, P. et al. Response of osteoblasts to low fluid shear stress is time dependent. *Tissue Cell* 43, no. 5 (2011): 311-317. doi: 10.1016/j.tice.2011.06.003.
26) N.H. Hart, R.U. Newton, J. Tan, T. Rantalainen, P. Chivers, A. Siafarikas, S. Nimphius. Biological basis of bone strength: anatomy, physiology and measurement. *The Journal of Musculoskeletal and Neuronal Interactions* 20, no. 3 (2020): 347-371.
27) N. H. Hart, S. Nimphius, T. Rantalainen, A. Ireland, A. Siafarikas, R. U. Newton. Mechanical basis of bone strength: Influence of bone material, bone structure and muscle action. *The Journal of Musculoskeletal and Neuronal Interactions* 17, no. 3 (2017): 114-139.
28) M. Wall, D. Butler, A. El Haj, J.C. Bodle, E.G. Loboa, A.J. Banes. Key developments that impacted the field of mechanobiology and mechanotransduction. *Journal of Orthopedic Research* 36, no. 2 (2018): 605-619. doi: 10.1002/jor.23707
29) Amengual-Peñafiel L, Brañes-Aroca M, Marchesani-Carrasco F, Jara-Sepúlveda MC, Parada-Pozas L, Cartes-Velásquez R. Coupling between osseointegration and mechanotransduction to maintain foreign body equilibrium in the long-term: A comprehensive overview. *Journal of Clinical Medicine* 8, no. 2 (2019): 139. doi: 10.3390/jcm8020139.

30) C. Argentati, F. Morena, I. Tortorella, M. Bazzucchi, S. Porcellati, C. Emiliani, et al. Insight into mechanobiology: how stem cells feel mechanical forces and orchestrate biological functions. *International Journal of Molecular Science* 20, no. 21 (2019): 5337. doi: 10.3390/ijms20215337.

31) C. Falcinelli, F. Valente, M. Vasta, T. Traini. Finite element analysis in implant dentistry: State of the art and future directions. Dental Materials 39, no. 6 (2023): 539-556. doi: 10.1016/j.dental.2023.04.002.

32) D. D’Andrea, A. Pistone, G. Risitano, D. Santonocito, L. Scappaticci, F. Alberti. Tribological characterization of a hip prosthesis in Si_3N_4-TiN ceramic composite made with Electrical Discharge Machining (EDM). *Procedia* Structural *Integrity* 33 (2021): 469–81.

33) M.A. Bianchini, N.B. Junior, B.A. Dedavid, P.N. De Aza, S.A. Gehrke. Comparative analysis of the mechanical limits of resistance in implant/abutment set of a new implant design: An in vitro study. *PLoS One* 18, no. 1 (2023): e0280684. doi: 10.1371/journal.pone.0280684.

Legends Figures

Figure 1. Illustrations of TA in different settings

Figure 2. Models and Components : a) TA Ti and b) TA CERAMIC

Figure 3. Stress and strain distribution in the bone structure under (a) axial loading and (b) oblique.

Figure 4. Force application points (a) and mesh convergence of the models under oblique loading (b, c) and axial loading (d, e).

Figure 5. Clinical and radiographic presentation of the use of TA Ti in an 10-year follow-up.

Table 1. Material properties used in the FEA

Young's modulus (E); Poisson's ratio (ν); Tensile yield strength (σyt); Compressive yield strength (σyc); Yield strength values (Fy) for ductile Materials

AXIAL LOADS – 250 N

Structures	**TA CERAMIC**	**TA Ti**	**% Increase**
Implant	520,9	450,62	15%
Mini abutment / UCLA	412,1	370,5	11%
Screw	229,7	202,6	13,4%
TA	40,4	39,8	1,5%

OBLIQUE LOADS - 100 N

Structures	**TA CERAMIC**	**TA Ti**	**% increase**
Implant	644,7	590,6	9,2%
Mini abutment / UCLA	*576,8*	521,0	10,7%
Screw	328,9	275,0	19,6%
TA	55,9	56,9	1,7%

Table 2: Maximum stresses in prosthetic components structures (in MPa)

Young's modulus (E); Poisson's ratio (ν); Tensile yield strength (σyt); Compressive yield strength (σyc); Yield strength values (Fy) for ductile materials

Models and components	***E [GPa]***	ν	σyt ***[Mpa]***	σyc ***[Mpa]***	***- Fy [Mpa]***
Cancellous bone	1,370	0,30	82,8	133,6	-
Cortical bone	13,7	0,30	82,8	133,6	-
Chrome cobalt alloy	218,0	0,33	-	-	560,0
Composite resin	7,6	0,24	-	-	-
Feldspathic porcelain	69,0	0,30	-	-	-
Ti-6Al-7Nb Alloy	105,0	0,36	-	-	800,00
ZrO2 (Y-TZP)	205	0,30	550	1200	-

Table 3: Stresses and micro-strains in the bone structure

AXIAL LOADS – 250 N			
Criteria	**TA CERAMIC**	**TA Ti**	**% increase**
Maximum Principal Stress [MPa]	42,8	41,7	2%
Minimum Principal Stress [MPa]	-264,20	-252,9	4,5%
Mohr-Coulomb Criterion	1,98	1,89	4,7%
Micro Strains [$\mu\varepsilon$]	13.864	13.378	3,6%
OBLIQUE LOADS - 100 N			
Criteria	**TA CERAMIC**	**TA Ti**	**% increase**
Maximum Principal Stress [MPa]	48,8	50,1	-2,5%
Minimum Principal Stress [MPa]	-303,1	-291,5	3,9%
Mohr-Coulomb Criterion	2,26	2,18	3,7%
Micro Strains [$\mu\varepsilon$]	16.097	15.342	4.9%

MPa = Megapascal

Table 4. Support reaction analysis across models

TA CERAMIC					
Axial loads	**Time step**	**Reaction in X [N]**	**REaction in Y [N]**	**Reaction in Z [N]**	**Total reaction [N]**
	1	-4,94E-11	4,62E-11	-6,96E-13	6,77E-11
	2	-34,499	-26,033	-246,23	249,99
Oblique loads	1	-3.16E-11	6,18E-11	-4,77E-11	8,42E-11
	2	34,825	-26,026	-90,051	99,997

TA Ti

	Time step	**Reaction in X [N]**	**REaction in Y [N]**	**Reaction in Z [N]**	**Total reaction [N]**
Axial loads	1	6,61E-10	1,57E-11	1,46E-11	6,61E-10
	2	-34,498	-26,033	-246,22	249,99
Oblique loads	1	-1,37E-10	-1,06E-10	7,20E-11	1,88E-10
	2	34,824	-26,025	-90,049	99,994

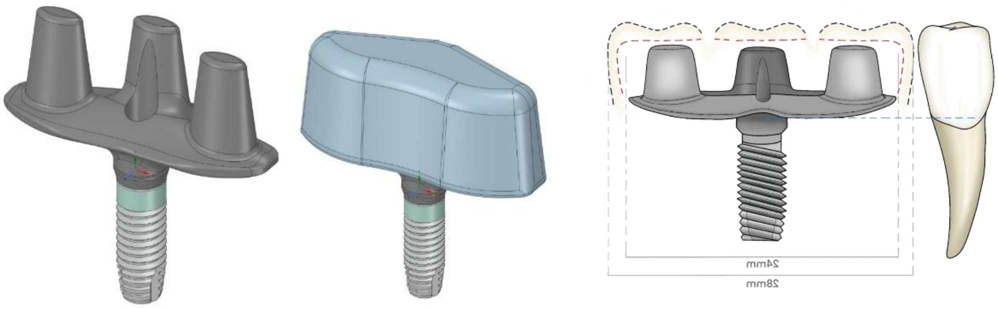

Figure 1. Illustrations of TA in different settings

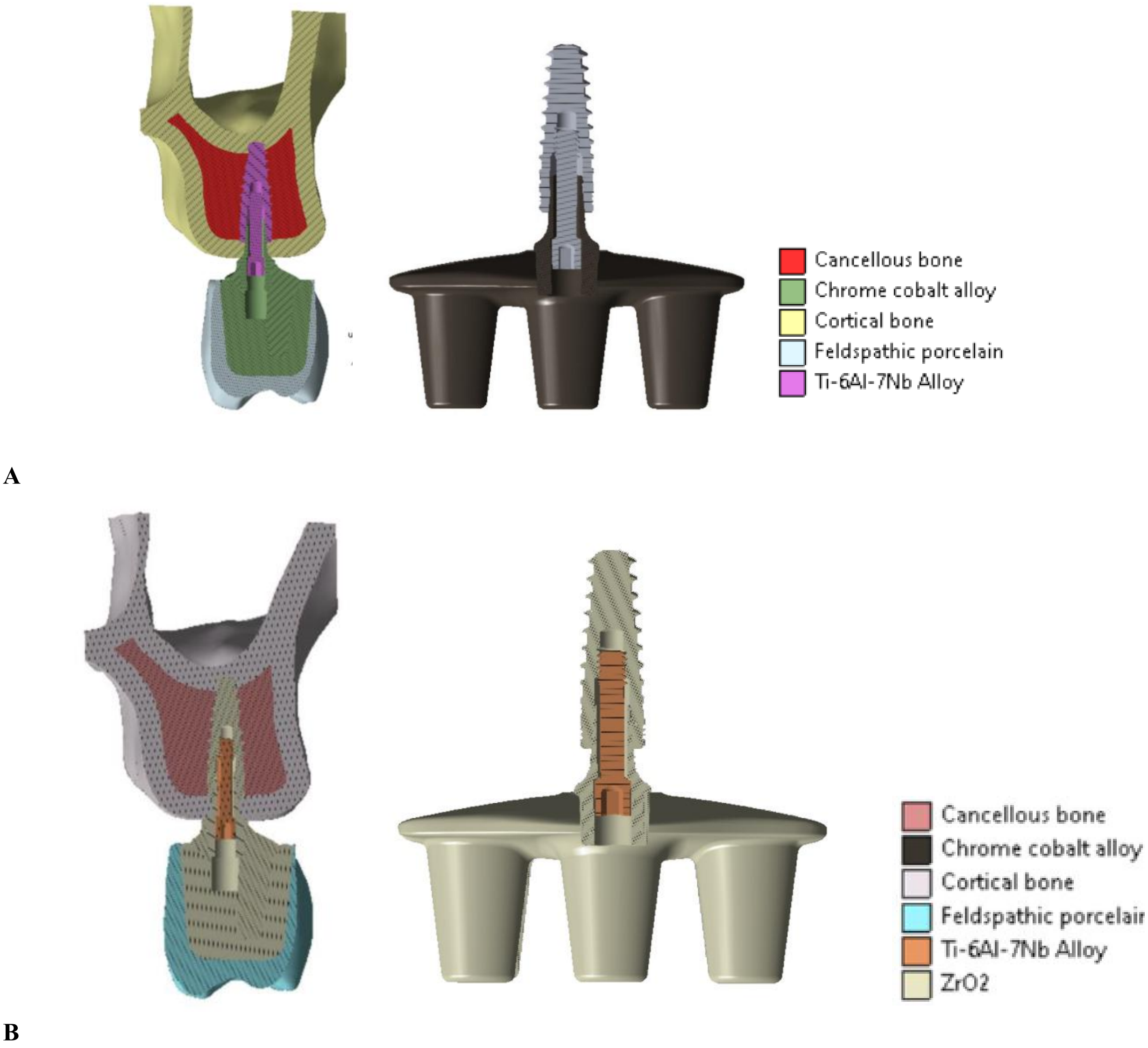

Figure 2. Models and Components : A) TA Ti and B) TA CERAMIC

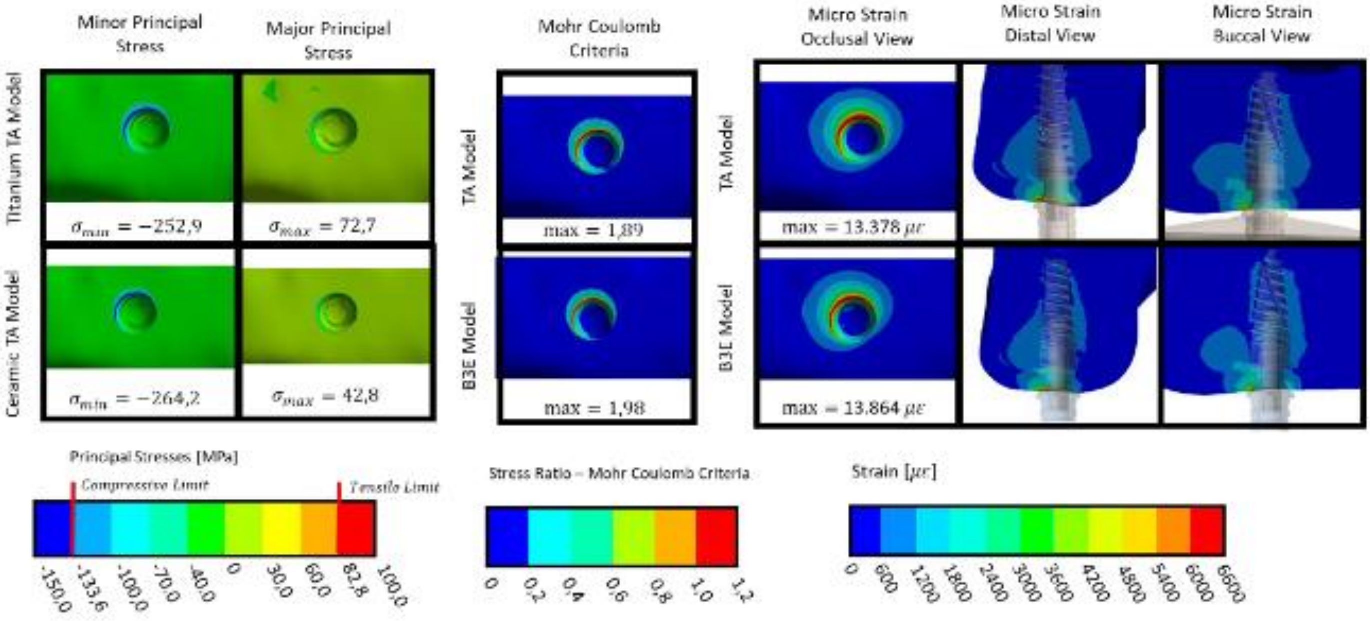

A

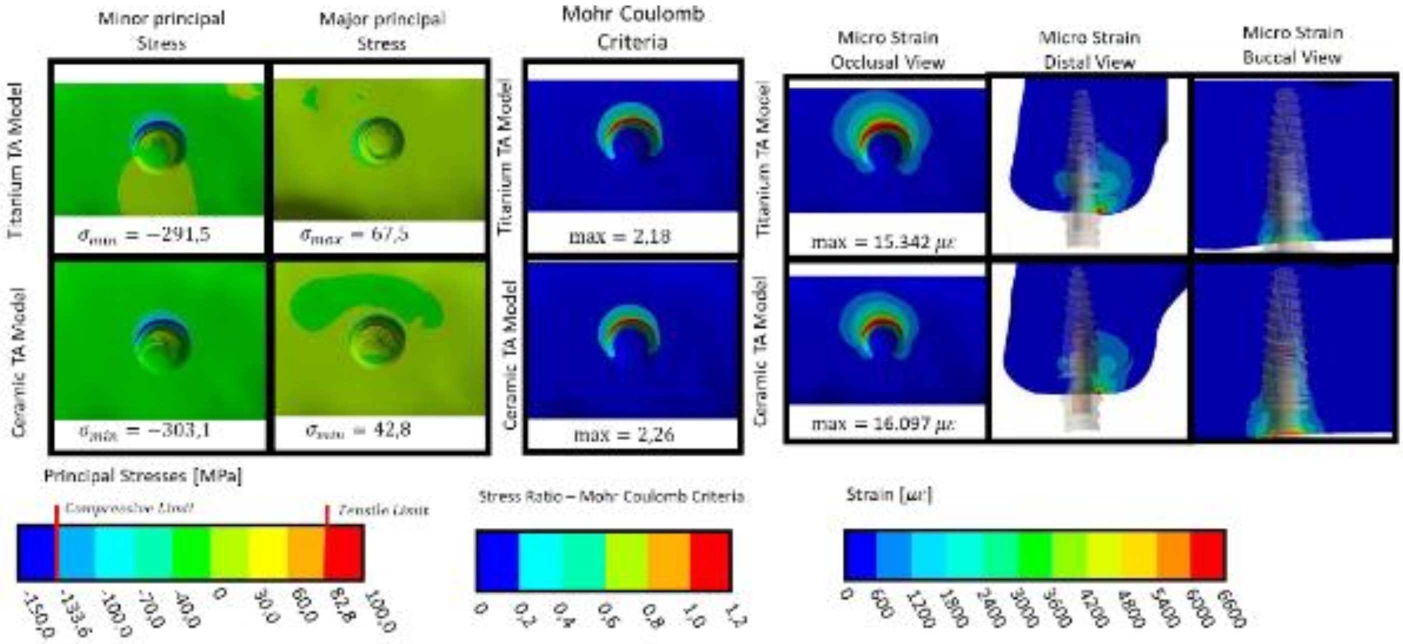

B

Figure 3. Stress and strain distribution in the bone structure under (A) axial loading and (B) oblique.

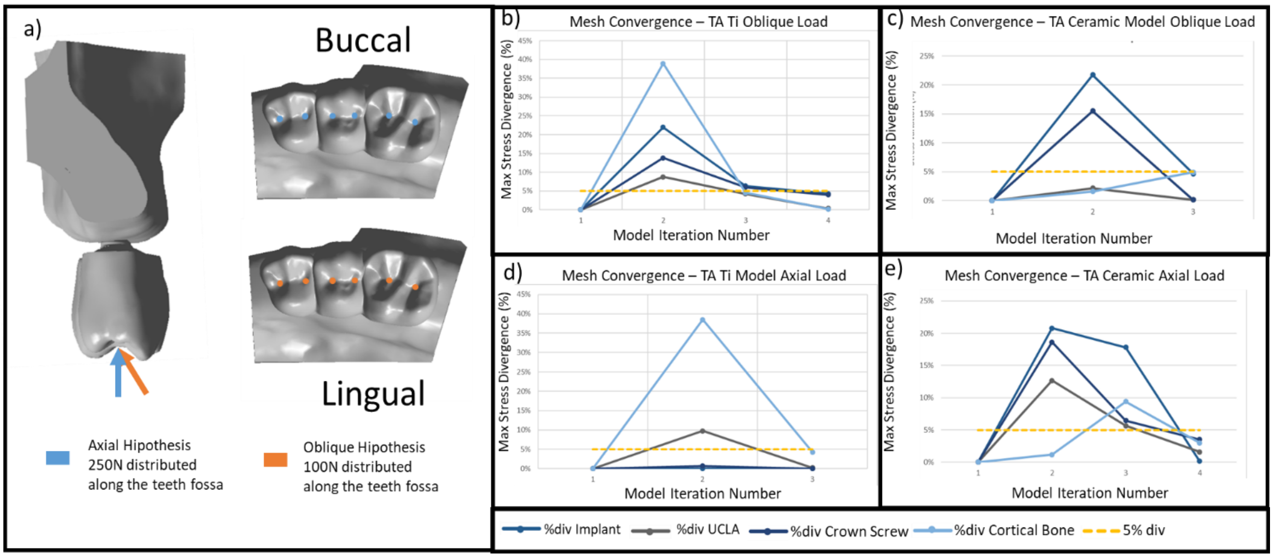

Figure 4. Force application points (a) and mesh convergence of the models under oblique loading (b, c) and axial loading (d, e).

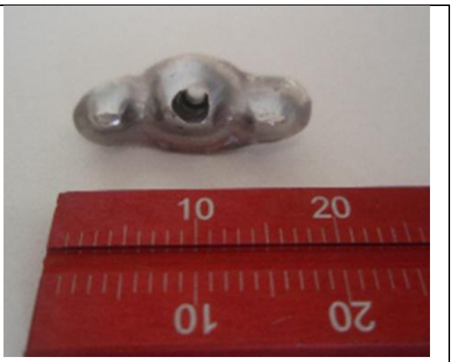

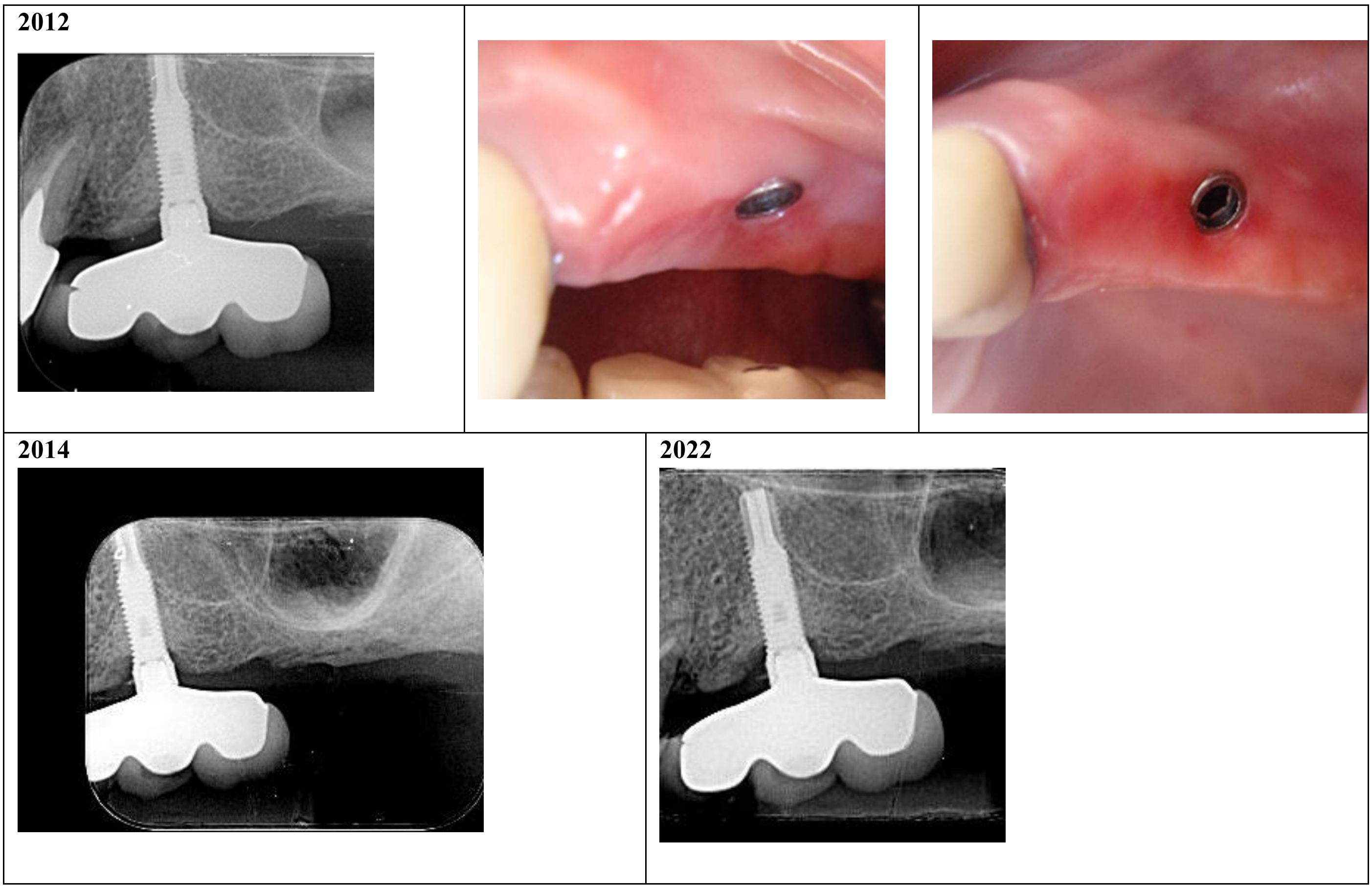

Figure 5. Clinical and radiographic presentation of the use of TA Ti in an 10-year follow-up.